

# Quantum inductance and negative electrochemical capacitance at finite frequency

Jian Wang \*,<sup>1</sup> Baigeng Wang,<sup>2</sup> and Hong Guo<sup>3</sup>

<sup>1</sup>*Center of theoretical and computational physics and Department of Physics,  
The University of Hong Kong, Pokfulam Road, Hong Kong, China*

<sup>2</sup>*Department of Physics, Nanjing University, Nanjing, China*

<sup>3</sup>*Department of Physics, McGill University, Montreal, Quebec, Canada*

We report on theoretical investigations of frequency dependent quantum capacitance. It is found that at finite frequency a quantum capacitor can be characterized by a classical RLC circuit with three parameters: a static electrochemical capacitance, a charge relaxation resistance, and a quantum inductance. The quantum inductance is proportional to the characteristic time scale of electron dynamics and due to its existence, the time dependent current can accumulate a phase delay and becomes lagging behind the applied ac voltage, leading to a negative effective capacitance.

PACS numbers: 72.10.-d, 73.23.-b, 73.21.La

Understanding dynamic conductance of quantum coherent conductors is a very important problem in nano-electronics theory. When two quantum coherent conductors form a double plate “quantum capacitor”, its dynamic conductance  $G(\omega)$  is given by the frequency dependent electrochemical capacitance<sup>1,2,3</sup>  $C_\mu(\omega)$ ,  $G(\omega) = -i\omega C_\mu(\omega)$ , here  $\omega$  is the frequency. At low frequency,  $C_\mu(\omega)$  can be expanded in frequency and at the linear order, it is described<sup>2</sup> by an equivalent classical circuit consisting of a static capacitor  $C_\mu$  in series with a “charge relaxation resistor”  $R_q$ . For a conductor having a single spin-resolved transmission channel,  $R_q$  was predicted<sup>2</sup> to be half the resistance quantum,  $R_q = 1/2G_o$  where  $G_o \equiv h/e^2$ . The factor 1/2 in  $R_q$  is of quantum origin<sup>2,4</sup>, and has recently been confirmed experimentally<sup>5</sup>. In the experiment of Gabelli *et.al.*<sup>5</sup>, a submicron 2DEG quantum dot (QD) is capacitively coupled to a gold plate forming a double plate capacitor, where the QD connects to the outside reservoir by a single channel quantum point contact (QPC). The dynamic conductance  $G(\omega)$  is then measured at 1.2GHz, and the data is well fit to the equivalent circuit characterized by two parameters ( $C_\mu, R_q$ ).

The experiment of Gabelli *et.al.*<sup>5</sup> opened the door for elucidating important and interesting physics of high frequency quantum transport in meso- and nano-scale devices. An important question is what happens to electrochemical capacitance at higher frequencies beyond the linear  $\omega$  regime, and in particular whether the two-parameter ( $C_\mu, R_q$ ) equivalent circuit is adequate at higher frequencies to describe a quantum capacitor. It is the purpose of this paper to address these issues.

In the following, we report a microscopic theory for high frequency quantum transport in a two-plate quantum capacitor. Our results show that to characterize its high frequency dynamic response, one needs—in addition to  $C_\mu, R_q$ , a new quantity  $L_q$  having the dimension of inductance.  $L_q$  is found to have purely quantum origin and will be named “quantum inductance”. Therefore, the frequency dependent electrochemical capacitance of a quantum capacitor  $C_\mu(\omega)$  is equivalent to a classical RLC circuit characterized by three parameters ( $C_\mu, R_q, L_q$ ), at

high frequency. Due to  $L_q$ , electrons dwell in the neighborhood of the capacitor plates causing a phase delay. At low frequencies, the dynamic response is capacitive-like and voltage lags current. At larger frequencies when  $\omega > 1/\sqrt{C_\mu L_q}$ , inductive behavior dominates and voltage leads current: in this case the quantum capacitor gives a negative capacitance value. It is, indeed, surprising that a quantum capacitor can give an inductive dynamic response. For the experimental setup of Ref.5, we estimate that when  $\omega \sim 3\text{GHz}$ , the predicted high frequency effects should be observable.

Let's first work out a simple expression for the frequency dependent electrochemical capacitance  $C_\mu(\omega)$  following the work of Buttiker<sup>2</sup>. We consider a two-plate capacitor similar to the experiment of Gabelli *et.al.*<sup>5</sup>: a QD—labelled I, and a large metallic electrode—labelled II. Each plate is connected to the outside world through its lead and a time dependent bias  $v_{1,2}$  is applied across the two leads. We consider small amplitudes of  $v_{1,2}$  so as to focus on the linear bias regime. Under the action of such a bias, the two capacitor plates develop their own frequency dependent electric potential  $U_{I,II}(\omega)$ . The charge on plate-I is equal to the sum of the injected charge and induced charge:  $Q_I = Q_I^{inj} + Q_I^{ind}$ . In the linear regime, the injected charge is proportional to bias  $v_1(\omega)$ :  $Q_I^{inj} = e^2 D_I(\omega) v_1(\omega)$  where  $D_I(\omega)$  is the generalized global density of states (DOS) of plate-I at frequency  $\omega$ . The induced charge, on the other hand, is in general related to a nonlocal Lindhard function<sup>2</sup> whose calculation is simplified by applying the Thomas-Fermi approximation. Within this approximation, the induced charge is proportional to the induced potential  $U_I$  on the plate:  $Q_I^{ind} = -e^2 D_I(\omega) U_I$  where the minus sign indicates that the charge is induced. Putting things together, we obtain  $Q_I = e^2 D_I(\omega) (v_1 - U_I)$ . Clearly, the same charge  $Q_I$  can be calculated by the usual electrostatic geometric capacitance  $C_o$ :  $Q_I = C_o (U_I - U_{II})$ . We therefore obtain a relationship:  $C_o (U_I - U_{II}) = e^2 D_I(\omega) (v_1 - U_I)$ . Applying the same argument to plate-II, we similarly obtain  $-C_o (U_I - U_{II}) = e^2 D_{II}(\omega) (v_2 - U_{II})$ . Finally, the same charge  $Q_I$  can also be obtained from the definition of the electrochemical capacitance:  $Q_I = C_\mu(\omega) (v_1 - v_2)$ .

These three relations allow one to derive the following expression for  $C_\mu(\omega)$ :

$$\frac{e^2}{C_\mu(\omega)} = \frac{e^2}{C_o} + \frac{1}{D_I(\omega)} + \frac{1}{D_{II}(\omega)} \quad (1)$$

This result resembles the one obtained by Büttiker for the static capacitance<sup>2</sup>. An important difference is that the frequency dependent electrochemical capacitance in Eq.(1) is a complex quantity: its real part is a measure to the electrochemical capacitance and its imaginary part is proportional to the frequency dependent charge relaxation resistance.

To proceed further, we need to calculate the frequency dependent DOS  $D_{I,II}(\omega)$ . Following Ref.4, the generalized local DOS of plate- $\alpha$  of the capacitor can be expressed in terms of Green's functions:

$$\frac{dn_\alpha(\omega)}{dE} = \int \frac{dE}{2\pi} \frac{f - \bar{f}}{\hbar\omega} [\bar{G}^r \Gamma_\alpha G^a]_{xx} \quad (2)$$

where the subscript  $x$  labels space coordinates and  $D_\alpha(\omega) = Tr[dn_\alpha(\omega)/dE]$ . In Eq.(2),  $f$  is the Fermi function and  $\bar{f} \equiv f(E_+)$  with  $E_+ \equiv E + \hbar\omega$ ;  $G^{r,a} = G^{r,a}(E)$  is the retarded/advanced Green's function at energy  $E$  and  $\bar{G}^r \equiv G^r(E + \hbar\omega)$ ;  $\Gamma_\alpha$  is the linewidth function describing the coupling strength between plate- $\alpha$  with its lead. These quantities can be calculated in straightforward manner when the Hamiltonian of the capacitor model is specified<sup>6,7</sup>.

For the quantum capacitor of Ref.5, plate-I is a QD and plate-II is a metal gate. Since the metal gate has much greater DOS, *i.e.*  $D_{II} \gg D_I$ , we can safely neglect the  $D_{II}$  term in Eq.(1). For a QD with one energy level  $E_0$  and connected to one lead, its Green's function  $G^r = 1/(E - E_0 + i\Gamma_L/2)$  where  $\Gamma_L$  is the linewidth function of the lead. With this Green's function, the frequency dependent DOS can be easily calculated from Eq.(2), we obtain:

$$D_I(\omega) = \frac{\Gamma_L}{2\pi\hbar\omega(\hbar\omega + i\Gamma_L)} \left[ \frac{1}{2} \ln \frac{\Delta^2}{\Delta_+ \Delta_-} - i \left( \arctan \frac{\Delta E - \hbar\omega}{\Gamma_L/2} - \arctan \frac{\Delta E + \hbar\omega}{\Gamma_L/2} \right) \right] \quad (3)$$

where  $\Delta = \Delta E^2 + \Gamma_L^2/4$ ,  $\Delta_\pm = (\Delta E \pm \hbar\omega)^2 + \Gamma_L^2/4$ , and  $\Delta E = E_F - E_0$ . At resonance  $\Delta E = 0$ , we obtain  $Re(D_I(\omega)) = [-x \ln(4x^2 + 1) + 2 \arctan(2x)]/(2\pi\Gamma_L x)/(x^2 + 1)$  with  $x = \hbar\omega/\Gamma_L$ . Hence  $Re(D_I(\omega))$  is positive for small  $x$  and negative for large  $x$ , *i.e.* there is a sign change. A similar behavior is also found for the system away from the resonance. Due to this sign change of  $Re(D_I)$ , from Eq.(1) the frequency dependent electrochemical capacitance  $C_R \equiv Re[C_\mu(\omega)]$  can become negative.

To be more specific, we fix the classical capacitance of QD  $C_0 = 1\text{fF}$  which is a typical value for QD with area of  $\sim 1\mu\text{m}^2$ . Fig.1 plots  $C_R = Re[C_\mu(\omega)]$  (real part) and  $C_I = Im[C_\mu(\omega)]$  (imaginary part) versus frequency

for different values of  $\Gamma_L$ , by setting  $\Delta E$  and temperature to zero. We observe that  $C_R$  is positive at small frequency and becomes negative at larger frequency. For instance,  $C_R$  becomes negative at a "critical" frequency  $\omega_c \sim 10\text{GHz}$  for  $\Gamma_L = 10\mu\text{eV}$ . This critical frequency can be smaller for smaller linewidth function  $\Gamma_L$ . We note that it is not difficult to achieve  $\Gamma_L = 10\mu\text{eV}$  experimentally: in Ref.8,  $\Gamma_L$  between  $1\mu\text{eV}$  to  $5\mu\text{eV}$  has been realized. As will be discussed below, the effective  $\Gamma_L$  in the experiment of Ref.5 is tunable by a gate voltage so that the critical frequency at which the negative capacitance occurs can be even smaller. The inset of Fig.1 also shows that as we increase  $\omega$ , the imaginary part of  $C_\mu(\omega)$  starts from zero, reaches a peak value around  $\omega_c$  and then decays to zero. The negative capacitance at large frequency can be understood as follows. For a classical capacitor, a charge is accumulated across the capacitor induced by an external voltage. The current and voltage has a fixed phase relationship: the voltage lags behind current with a phase  $\pi/2$ . For a quantum capacitor at low frequency, there exists a charge relaxation resistance  $R_q = h/(2e^2)$  for a single channel plate, therefore the charge build-up time is the RC-time  $\tau_{RC} = R_q C_\mu$ . For  $C_\mu = 1\text{fF}$  and  $R_q = h/(2e^2)$ , this RC-time is about  $\tau_{RC} = 13\text{ps}$ . If the external voltage reverses sign, the charge accumulation will follow the voltage and also reverse sign in due time. When frequency is low, namely when  $\omega \ll 1/\tau_{RC} = 77\text{GHz}$ , the charge build up follows the ac bias almost instantaneously just like a classical capacitor, thus the capacitance is positive. When frequency is high, there is a phase difference between the ac bias and the charge build up. For frequencies comparable to  $1/\tau_{RC}$ , the charge build up can not follow the ac bias, thereby the capacitance may be negative.

While the above argument explains why it is possible to have negative capacitance, it would indicate a critical frequency to be near  $77\text{GHz}$ . Our results (Fig.1) show that the calculated  $\omega_c$  is actually much smaller. This is because there exists a second relevant time scale in the QD, *i.e.* the dwell time  $\tau_d$  which is the time spent by electrons inside the QD. The dwell time  $\tau_d$  can be calculated for specific systems<sup>9</sup>. Importantly, at resonance the electrons can dwell inside the quantum dot for a long time. For instance, for our QD with  $\Gamma_L = 10\mu\text{eV}$ , we found  $\tau_d = 260\text{ps}$  while  $\tau_{RC} = 12\text{ps}$  (since  $C_\mu = 0.9\text{fF}$ ). In other words,  $\tau_d \gg \tau_{RC}$ . Such a  $\tau_d$  corresponds to a frequency of  $4\text{GHz}$ , much less than  $1/\tau_{RC}$ . In other words, when ac frequency is greater than  $1/\tau_d$ , the charges dwell inside the quantum dot and cannot respond to the ac voltage change. As a result, current becomes lagging behind voltage, leading to a negative capacitance. This picture agrees very well with the numerical results (Fig.1).

Having determined the general behavior of  $C_\mu(\omega)$  for the quantum capacitor, in the following we determine how to simulate this quantity using a classical circuit. Expanding Eq.(1) into a Taylor series to second order in

$\omega$  with the help of Eq.(3) at resonance, we obtain:

$$C_\mu(\omega) = C_\mu + i\omega C_\mu^2 \frac{h}{2e^2} - \omega^2 C_\mu^3 \frac{h^2}{4e^4} + \omega^2 C_\mu^2 \frac{h^2}{12\pi\Gamma_L e^2} \quad (4)$$

where  $C_\mu = C_\mu(0)$  on the right hand side is the static electrochemical capacitance. This result is equivalent to that of a classical RLC circuit, as follows. For a classical RLC circuit with capacitance  $C_\mu$ , resistance  $R_q$  and inductance  $L_q$ , the dynamic conductance is

$$G(\omega) = -i\omega C_\mu / (1 - \omega^2 L_q C_\mu - i\omega C_\mu R_q) \quad (5)$$

Expanding this expression in power series of  $\omega$ , we obtain

$$G(\omega) = -i\omega C_\mu + \omega^2 C_\mu^2 R_q + i\omega^3 C_\mu^3 R_q^2 - i\omega^3 C_\mu^2 L_q \quad (6)$$

Because for a capacitor  $G(\omega) = -i\omega C_\mu(\omega)$ , we obtain the result that our quantum capacitance Eq.(4) is equivalent to the classical RLC circuit model of Eq.(6). Comparing these two equations we readily identify  $R_q = h/(2e^2)$ —a result first obtained by Büttiker and co-workers<sup>2</sup>. Importantly, a new quantity—the equivalent inductance, is identified as  $L_q = h^2/(12\pi e^2 \Gamma_L)$ . In terms of dwell time  $\tau_d$  and charge relaxation resistance  $R_q$ , we obtain:

$$L_q = R_q \tau_d / 12 \quad (7)$$

where  $\tau_d = 4\hbar/\Gamma_L$ .

What is the reason that a quantum capacitor at finite frequency needs to be modeled by a classical RLC circuit (instead of a RC circuit)? This is due to the role played by the large dwell time  $\tau_d$  of the QD. When electrons dwells a long time  $\tau_d$  inside the QD, the interaction between electrons become an important piece of physics which, in our theory, is modeled by the induced self-consistent potential  $U_{I,II}$  discussed above. Such an interaction gives rise to the physics of induction, and resulting to the quantity  $L_q$  of Eq.(7). Indeed, the explicit dependence on  $\tau_d$  by  $L_q$  also confirms the important role played by the dwell time. Because  $L_q$  is determined by  $\tau_d$  as well as fundamental constants  $\hbar$  and  $e$ , it is of purely quantum origin and can be called quantum inductance.

Fig.2 compares the fitting of classical RLC circuit Eq.(5), with the full quantum result of Eq.(1). They compare very well for the entire range of the frequency—if we treat  $R_q$  as a function of  $\omega$ . Indeed, while  $R_q$  has so far been a constant  $h/(2e^2)$  as identified through the Taylor expanded Eqs.(4,6), it is actually a function of  $\omega$  by the more general expression Eq.(5). The inset of Fig.3 plots the general  $R_q = R_q(\omega)$  obtained numerically, and we observe it to be a slowly increasing function of  $\omega$ . As expected, in the small frequency limit,  $R_q(\omega)$  recovers the result of half resistance quantum. For  $\Gamma_L = 50\mu eV$ ,  $R_q(\omega)$  deviates from  $h/2e^2$  at about  $5GHz$ . We have also attempted using three *constant* parameters  $C_\mu$ ,  $L_q$  and  $R_q = h/(2e^2)$  into Eq.(5) to compare with the full quantum result of Eq.(1), a reasonable agreement is obtained (inset of Fig.2) although not as good as that shown in Fig.2.

The situation is somewhat different for quantum inductance  $L_q$  when the system is *off* resonance ( $\Delta E \neq 0$  in Eq.(3)). In this case the dwell time  $\tau_d$  becomes too small to be relevant and another time scale becomes important, namely the tunneling time  $\tau_t$  for electrons to go in/out of the QD. The further away  $E$  is from  $E_0$ , the longer is  $\tau_t$ . Hence in Eq.(7)  $\tau_d$  should be replaced by  $\tau_t$  for off resonance. Our result shows that the fitting of full quantum capacitance  $C_\mu(\omega)$  using classical parameters  $C_\mu$ ,  $L_q$  and  $R_q(\omega)$  is still quite good for off resonance. This further supports the conclusion that the frequency dependent quantum capacitance can be described by a classical RLC circuit with static electrochemical capacitance, charge relaxation resistance, and a quantum inductance.

Finally, we perform a numerical calculation of the dynamic conductance for the device structure of Ref.5. In terms of scattering matrix, the DOS of Eq.(2) for a capacitor can be re-written as<sup>4,6</sup>

$$D_I(\omega) = i \int \frac{dE}{2\pi} \frac{f - \bar{f}}{\hbar^2 \omega^2} [1 - s_{LL}^\dagger(E_+) s_{LL}(E)] \quad (8)$$

with<sup>5</sup>  $s_{LL}^\dagger(E) = (r - e^{i\phi})/(1 - re^{i\phi})$ ,  $\phi = 2\pi E/\Delta$ ,  $r^2 = 1 - T_{QPC}$  and  $T_{QPC} = 1/[1 + \exp(-(V_g + V_0)/\Delta V_0)]$  which is the transmission coefficient of the QPC in the experimental setup<sup>5</sup>. Fig.3 shows the dynamic conductance  $G(\omega)$  vs gate voltage  $V_g$  using our theory presented above. When  $\omega = 1.2GHz$  (open circle), our results agrees very well<sup>10</sup> with the experimental data of Ref.5. When  $\omega = 3GHz$  (open square), our theory predicts that the imaginary part of  $G(\omega)$  which is the electrochemical capacitance, goes to negative. For even larger frequency  $\omega = 5GHz$  the effect is more significant. To understand why one can observe a negative capacitance at small frequency such as  $3GHz$ , we note that since electron entering the QD has to first pass the QPC<sup>5</sup>: this QPC serves as a barrier (with an effective barrier height  $1/\Gamma$ ) that is controlled by the gate voltage. At small gate voltage,  $T_{QPC}$  is nearly zero and goes to one at large  $V_g$ . Hence the effective  $\Gamma$  for small gate voltage is quite large making  $\omega_c$  much smaller. Since the experiment of Ref.5 is performed at  $\omega = 1.2GHz$ , we assume that it is not too difficult to push the frequency to  $3GHz$  so that the effect of quantum inductance can be observed experimentally. Indeed, a single-wall carbon nanotube transistor operated at  $2.6GHz$  has been demonstrated<sup>11</sup> and measurement of current fluctuation at frequency from 5 to 90 GHz has been reported<sup>12</sup>.

In summary, we found that at finite frequency, a quantum capacitor consisting of a quantum dot and a large metal conductor is equivalent to a classical RLC circuit with three basic parameters: a static electrochemical capacitance  $C_\mu$ , a charge relaxation resistance  $R_q$ , and a quantum inductance  $L_q$ . It is found that  $L_q \sim R_q \tau$  where  $\tau$  is the characteristic time scale for the quantum dot such as the dwell time  $\tau_d$  or the tunneling time  $\tau_t$ . Due to the phase delay by the quantum inductance, the dynamic current can lag behind of the applied ac voltage, giv-

ing rise to a negative capacitance. Our numerical results show that this effect should be detectable experimentally using the present device technology.

**Acknowledgments.** We thank Prof. K. Xia for useful discussions. This work is supported by a RGC grant (HKU 7048/06P) from the HKSAR and LuXin Energy Group (J.W); NSF-China grant number 10474034

and 60390070 (B.G.W); NSERC of Canada, FQRNT of Québec and Canadian Institute of Advanced Research (H.G).

\*) Electronic address: jianwang@hkusub.hku.hk

FIG. 1: Frequency dependent capacitance  $C_\mu(\omega)$  versus frequency. Main figure is for  $C_R$  and inset is for  $C_I$ . Here  $\Gamma_L = 10\mu eV$  (for the curve with the open circle),  $50\mu eV$  (open square),  $100\mu eV$  (open triangle), and  $200\mu eV$  (open diamond). Here  $C_o = 1fF$ .

FIG. 2: Comparison of the full quantum capacitance  $C_\mu(\omega)$  (solid line) to that obtained by the classical RLC circuit model (dotted line) for  $\Gamma_L = 50\mu eV$ . Here  $Re[C_\mu(\omega)]$  is indicated by open circle. Inset: similar fit but using three constant parameters.

<sup>1</sup> S. Luryi, Appl. Phys. Lett. **52**, 501 (1998).

<sup>2</sup> M. Büttiker, J. Phys.: Condens. Matter **5**, 9361 (1993); M. Büttiker et al, Phys. Lett. A **180**, 364 (1993).

<sup>3</sup> T.P. Smith et al, Phys. Rev. B **32**, 2696 (1985).

<sup>4</sup> S.E. Nigg, R. Lopez and M. Büttiker, Phys. Rev. Lett **97**, 206804 (2006).

<sup>5</sup> J. Gabelli *et.al.*, Science **313**, 499 (2006).

<sup>6</sup> Z.S. Ma et al, Phys. Rev. B **59**, 7575 (1999).

<sup>7</sup> B.G. Wang et al, Phys. Rev. Lett. **82**, 398 (1999).

<sup>8</sup> T. Fujisawa *et.al.*, Science **282**, 932 (1998).

<sup>9</sup> V. Gasparian et al, Phys. Rev. A **54**, 4022 (1996).

<sup>10</sup> In classical RC circuit theory, the convention is writing  $v(t) = v_0 \exp(i\omega t)$ , while in quantum transport theory the convention is  $v(t) = v_0 \exp(-i\omega t)$ . This is responsible for the sign difference between our Fig.3 and the experimentally data of Ref.5.

<sup>11</sup> S.D. Li et al, Nano Lett. **4**, 753(2004).

<sup>12</sup> R. Deblock et al, Science **301**, 203(2003).

FIG. 3: The dynamic conductance  $G(\omega)$  (unit  $e^2/h$ ) versus gate voltage at different frequencies  $\omega = 1.2, 3, 5GHz$ . Solid line  $-Re[G]/\omega$ , dotted line  $-Im[G]/\omega$ . Other parameters:  $\Delta = 500mK$ ,  $\alpha = 3000$ ,  $V_0 = -0.85$ ,  $\Delta V_0 = 0.003$ ,  $C_0 = 4fF$ , and temperature  $50mK$ . For purpose of illustration, we divided  $G(\omega)$  by  $\omega$ . Inset: frequency dependent  $R_q$  (unit  $h/e^2$ ) vs frequency.

Fig1

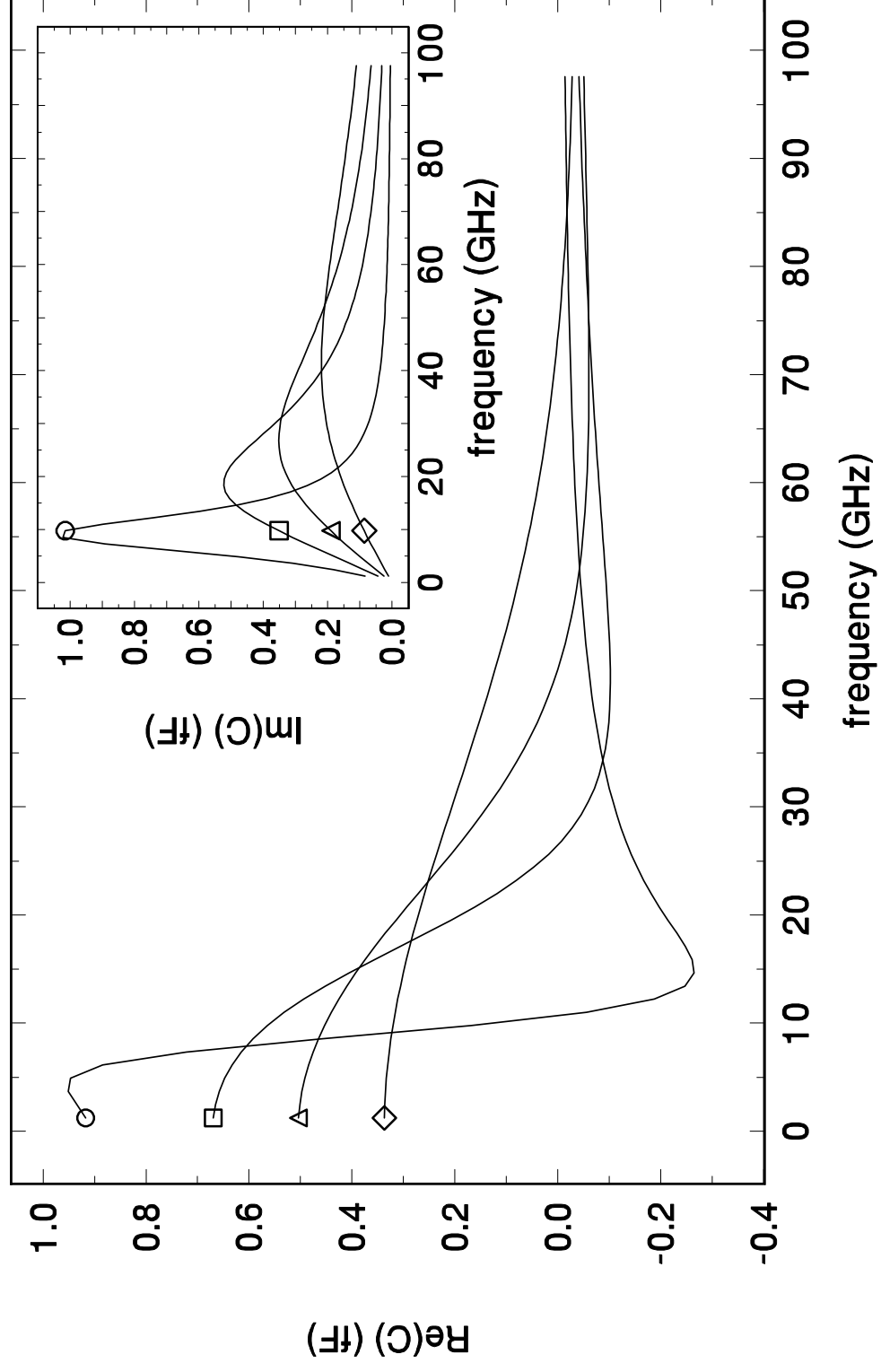


Fig2

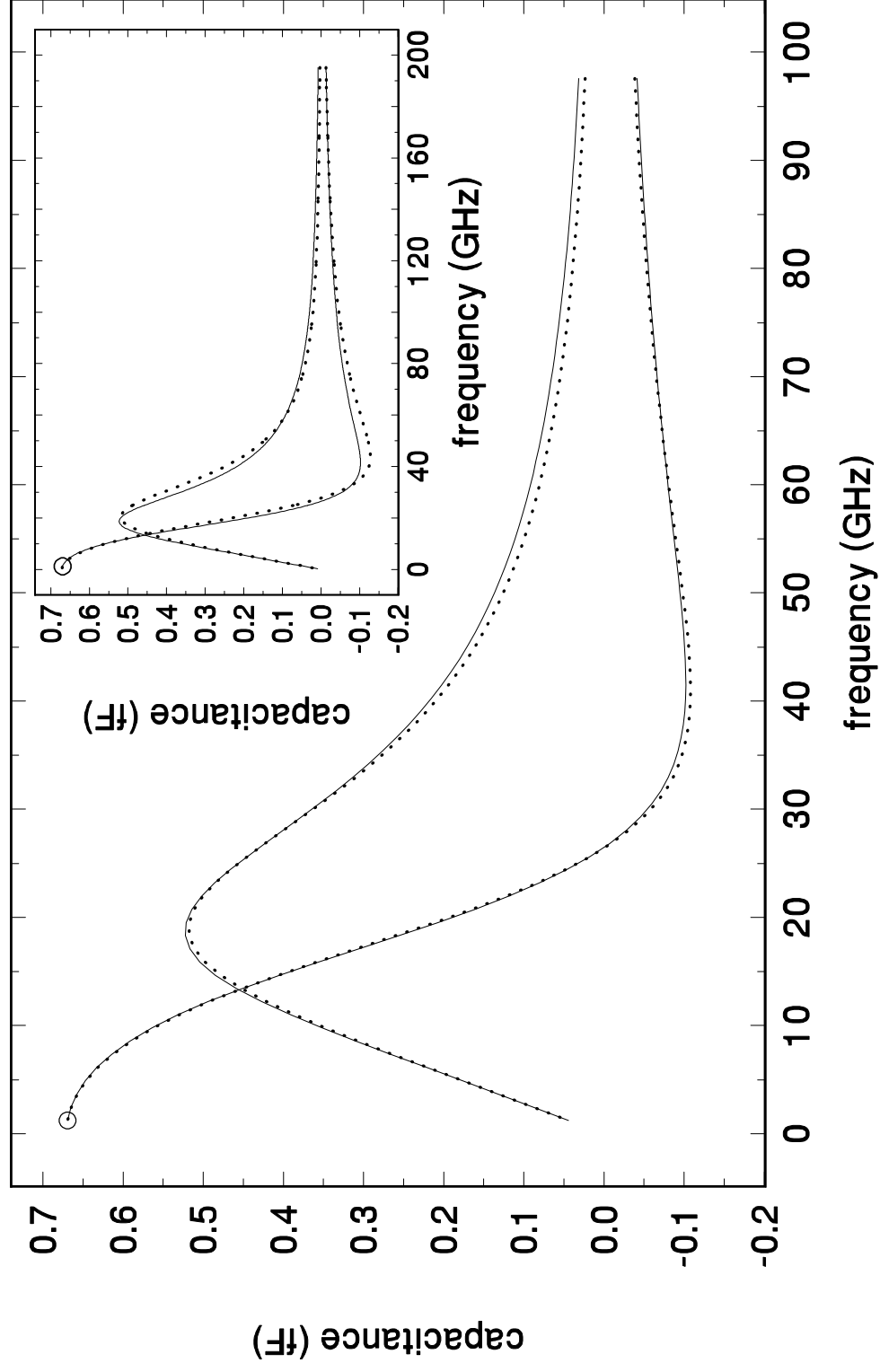


Fig.3

